Composites Part B 108 (2017) 377–385

Contents lists available at ScienceDirect

Composites Part B

journal homepage: www.elsevier.com/locate/compositesb

Tensile and bending behaviors and characteristics of laminated Ti-(TiBw/Ti) composites with different interface status

B.X. Liu [a, b, c], L.J. Huang [b, *], B. Kaveendran [b], L. Geng [b], X.P. Cui [b], S.L. Wei [b], F.X. Yin [a, c]

[a] Research Institute for Energy Equipment Materials, Hebei University of Technology, TianJin 300132, China
[b] School of Materials Science and Engineering, Harbin Institute of Technology, P.O. Box433, Harbin 150001, China
[c] TianJin Key Laboratory of Materials Laminating Fabrication and Interfacial Controlling Technology, China

ARTICLE INFO

Article history:
Received 29 March 2016
Received in revised form
17 September 2016
Accepted 2 October 2016
Available online 5 October 2016

Keywords:
Layered structures
Delamination
Damage mechanics
Fractography

ABSTRACT

A series of laminated Ti-(TiBw/Ti) composites fabricated at different diffusion welding temperatures of 1100 °C, 1200 °C and 1300 °C were subjected to tensile and bending tests. The results showed that the interfacial bonding strength, interfacial toughness and residual stress gradually increased with the increasing fabrication temperature. Therefore, along the transversal direction, the laminated composites fabricated at 1300 °C revealed the highest tensile strength and fracture elongation. However, the highest tensile strength (694 MPa) and elongation (22.7%) along the longitudinal direction, was recorded with the laminated composites fabricated at 1200 °C due to reasonable interfacial bonding and residual stress. Interestingly, the laminated composites fabricated at 1100 °C exhibited the highest bending fracture toughness and fracture work along arrester orientation. Due to the weak interfaces, the crack propagation path was displaced by delamination cracks and re-nucleated multiple tunnel cracks, which in turn lead to reduction in stress intensity of the main crack. This was beneficial to the toughening of the laminated Ti-(TiBw/Ti) composites.

1. Introduction

It is well known that titanium matrix composites (TMCs) are considered as suitable structural materials due to their special stiffness and strength. However, due to the addition of reinforcements, TMCs display low ductility and fracture toughness when compare to conventional Ti alloys, which prevents them from being used in a variety of applications [1–3]. Therefore, an optimized combination of strength and toughness of TMCs is expected to achieve before their potential applications can be fully realized. Recently, many new strategies have been employed to improve the toughness of metal matrix composites, such as network reinforcement distribution [4], gradient grain distribution [5] and laminated architecture [6].

Laminated architecture is a novel strategy to achieve high tensile ductility, fracture toughness and many other mechanical properties when compared to conventional materials [7,8]. It has been shown that the longitudinal tensile fracture elongation of laminated composites can be enhanced by introducing strong interfaces [9], it is because that strong and tough interfaces can effectively delay the localized necking of soft layers [10]. Generally, the enhanced fracture toughness of laminated composites can be attributed to two main extrinsic toughening mechanisms. One way of toughening is by inducing residual compressive stress, which occurs due to the mismatch in the coefficient of thermal expansion and elastic modulus between the different layers [11]. The other method is by introducing weak interfaces, which can induce low energy paths for crack propagation. Interfacial delamination crack is one of most important toughening methods for multilayered composites [12].The delamination crack may propagate along the weak interfaces ahead of the main crack tip, resulting in a reduction and redistribution of local stress [13,14]. Both of the extrinsic toughening methods always result in the decreasing local stress intensity in the laminated composites.

In our previous work [7,15], the tensile properties of laminated Ti-(TiBw/Ti) composites with strong interfaces were investigated in detail, revealing high strength and superior fracture elongation. Actually, the mechanical properties of laminated Ti-TiBw/Ti composites can be affected by many structural parameters, such as laminated, network, TiBw and interface structures. The tensile behavior of laminated Ti-TiBw/Ti composites with different

* Corresponding author.
E-mail address: huanglujun@hit.edu.cn (L.J. Huang).

http://dx.doi.org/10.1016/j.compositesb.2016.10.001
1359-8368/

fabrication method [16], layer thicknesses [17], layer thickness ratio [18] and volume fraction of TiB reinforcement [19,20] have been reported in the previous work. It is revealed that the laminated Ti-TiBw/Ti composite is a potential candidate for applications in structural materials. However, laminated composites should be formed in further process such as cutting, forging, rolling, bending and joining. Uscinowicz et al. reported moderate interfacial bonding strength is necessary for laminated composites to inhibit the interfacial delamination phenomenon during the forming process [21–24]. Sheng et al. [25,26] proposed that the fabrication parameters (temperature, rolling passes) can obviously affect the interfacial bonding status. Otherwise, laminated composites are always subjected to various stress states during the service process. Therefore, the further investigation of the different deformation modes (tensile and bending) of the laminated Ti-(TiBw/Ti) composites with different diffusion welding temperatures may prove useful to understand the relationship between structure and performance. The results could be used as guide to design microstructures and improve the mechanical properties of composites.

2. Experimental procedures

The laminated Ti-(TiBw/Ti) composites are comprised of alternatively stacked Ti layers and TiBw/Ti composite layers with layer thickness of 200 μm. The process essentially involved two steps: the preparation of the as-sintered 8 vol % composites with a network microstructure followed by diffusion bonding of the Ti to the (TiBw/Ti) to form the laminated Ti-(TiBw/Ti) composites.

Fig. 1 shows the fabrication process of the laminated Ti-TiBw/Ti composites by diffusion welding. Firstly, in order to form a network distribution of reinforcements, the fine prismatic TiB_2 (3~5 μm) powders were made to uniformly adhere to the surface of the large titanium powders (~100 μm) by low energy ball milled under a pure Ar atmosphere with a speed of 150 rpm for 5 h. The mixed powders were subsequently taken in a graphite mold and hot pressed in a vacuum (10^{-2}Pa) at 1200 °C under a pressure of 25 MPa for 40min in order to obtain bulk TiBw/Ti composites with a network microstructure. The TiB phase was in situ synthesized according to the following reaction:

$$Ti + TiB_2 \rightarrow 2TiB \quad (1)$$

Based on the above reaction, 8 vol % composites with network reinforcement distribution were successfully fabricated. Then the as-sintered composites were cut into many sheets with a thickness of 200 μm using a wire-cut machine. Commercial pure Ti sheets (TA1) with 200 μm thickness were also selected. In order to clean the oil and contaminants on the surface of the of the pure Ti and TiBw/Ti composite sheets, the thin sheets were immersed for two minutes in a 2 vol % HF solution. They were subsequently cleaned with water, dried and alternatively stacked in a graphite mold with a number of 300. Finally, the stacked multilayered composites were hot pressed in a vacuum (10^{-2} Pa) with a heating rate of 10 °C/min. Holding temperatures of 1100 °C, 1200 °C and 1300 °C were used for 1 h along with a compaction pressure of 25 MPa to successfully fabricate the laminated composites by diffusion welding, and the final entire thickness of three laminated Ti-TiBw/Ti composites is about 59.0, 58.3 and 57.2 mm for 1100 °C, 1200 °C and 1300 °C, respectively. During the hot pressing process, the laminated Ti-TiBw/Ti with different interfacial status were successfully fabricated by diffusion welding. Obviously, the laminated Ti-TiBw/Ti composites show two-scale hierarchical structure: laminated structure in macro scale, and network structure in micro scale. Meanwhile, TiB phase displays a needle-like shape as shown in Fig. 1.

Microstructural examinations were performed using optical microscopy (OM) and scanning electron microscopy (SEM, Hitachi S-4700) on the laminated composites after etching using a 5% HF+15%HNO_3+80%H_2O solution. In order to attain a clear surface, the specimens were glued to a metallic plate and polished using a polishing machine. The tensile and bending test process was carried out using an instron-5500 electronic universal test machine at room temperature, in air, with a crosshead speed of 0.5 mm/min as

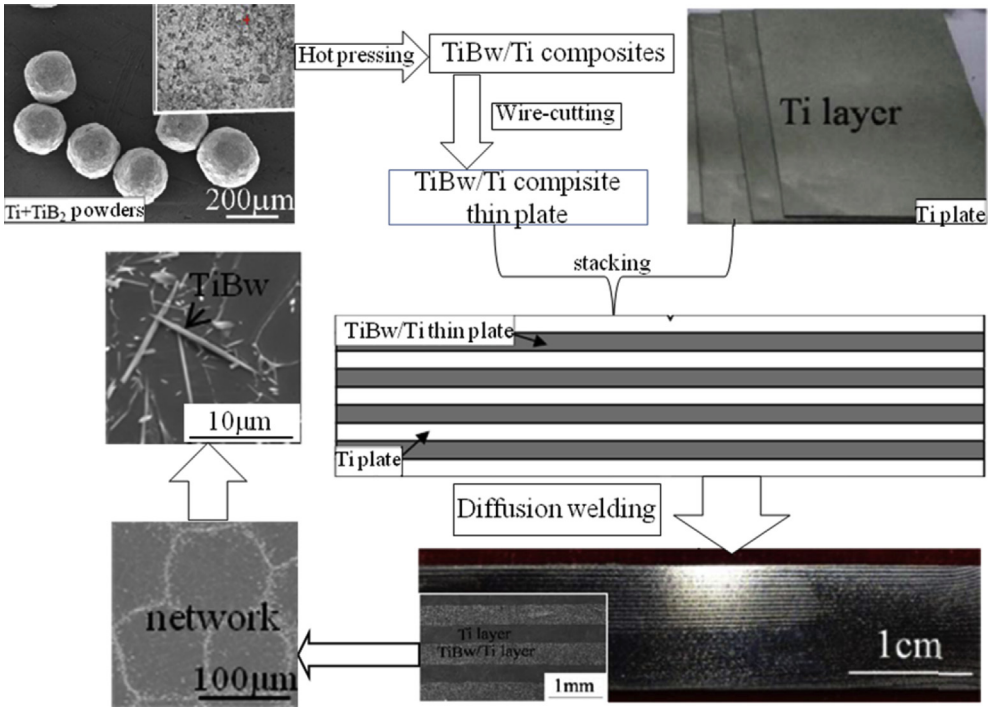

Fig. 1. The fabrication process of laminated Ti-TiBw/Ti composites by diffusion welding.

shown in Fig. 2. Tensile dog bone samples having dimensions of 18 mm × 5.6 mm × 2 mm were tested for each material as shown in Fig. 2a). The single-edge notched bend (SENB) specimens ($2 \times 4 \times 20$ mm^3) with a notched depth of 2 mm parallel to the loading direction is shown in Fig. 2b), which is in accordance with ASTM: E-399-09. A total of five samples were tested for each mode. The load-displacement (F-l) curve was acquired automatically by using an instron-5500 electronic universal test machine at room temperature. Assuming the maximum force, F_{max}, and the values of fracture toughness, characterized by K_{IC} and fracture energy (J) can be calculated by the following equations (2)–(4):

$$K_{IC} = \frac{F_{\max} L}{B^{\frac{1}{2}} W^{\frac{3}{2}}} \times f\left(\frac{a}{W}\right) \tag{2}$$

$$f\left(\frac{a}{W}\right) = 3\left(\frac{a}{W}\right)^{\frac{1}{2}} \times \frac{1.99 - \left(\frac{a}{W}\right)\left(1 - \frac{a}{W}\right)\left[2.15 - 3.93\left(\frac{a}{W}\right) + 2.70\left(\frac{a}{W}\right)^2\right]}{2\left(1 + \frac{2a}{W}\right)\left(1 - \frac{a}{W}\right)^{\frac{1}{2}}} \tag{3}$$

$$J = \frac{2\int Fdl}{B(W-a)} \tag{4}$$

where L, B, W, a are span, thickness, width of samples and the length of pre-crack (mm), respectively. The $f\left(\frac{a}{W}\right)$ is a geometry factor based on the dimension of specimen. In this work, $L = 16$ mm, $B = 2$ mm, $W = 4$ mm and $a = 2$ mm, respectively.

3. Results and discussions

Three kinds of laminated Ti-(TiBw/Ti) composites were fabricated at different diffusion welding temperatures as shown in Fig. 3. A weak interface between Ti and (TiBw/Ti) due to interfacial cracks and interfacial voids is present in the laminated composites fabricated at 1100 °C as shown in Fig. 3a). The diameter of voids is about 3~5 μm. At 1200 °C, a perfect interfacial bonding between the layers without pores or voids is evident as shown in Fig. 3b), and the laminated composites contain two scale hierarchical structures: laminated and network structures, which is reported in the previous work in detail [17]. Fig. 3c) shows the microstructure of laminated Ti-(TiBw/Ti) composites fabricated at 1300 °C, after etching, which reveal the presence of stress corrosion pores in the TiBw/Ti composite layer. The formation of these pores may be attributed to the etching process as well as the high residual stresses generated during the cooling process. Zuo et al. [27–29] reported that there exists residual radial tensile and compressive stress surrounding the reinforcement due to the mismatch of thermal expansion coefficients between Ti and TiBw, as well as the phase transition of Ti matrix. The residual thermal stress increases with increasing temperature, and the super-high residual tensile stress will easily bring some corrosion pores at the interfaces between Ti matrix and TiB reinforcements during slight etching process. In addition, the laminated composites fabricated at 1300 °C reveal wavy interface characteristics, which is a typical interfacial instability phenomenon proposed by Steif et al. [17,30–33], and Eizadjou et al. reported that Cu layer in the multi-layered A/Cu composite fabricated by accumulative roll bonding (ARB) process may be necked and fractured [34]. This phenomenon is attributed to the high deformation temperature and a high deformation reduction under the plane compression strain state according to bifurcation theory.

For the designed laminated structures, the estimation of the residual stress distribution of Ti layer and TiBw/Ti composite layer is necessary. The Ti layer is subject to residual tensile stress, whereas TiBw/Ti composite layer is subject to residual compression stress. The residual stress can be expressed as follows [11,35]:

$$\sigma_{Ti} = \frac{E_{Ti} \cdot E_{TiBw/Ti}\left(\alpha_{Ti} - \alpha_{TiB/Ti}\right) \cdot \Delta T}{\left(1 - \nu_{TiB/Ti}\right)E_{Ti} + (1 - \nu_{Ti})E_{TiBw/Ti}\lambda} \tag{5}$$

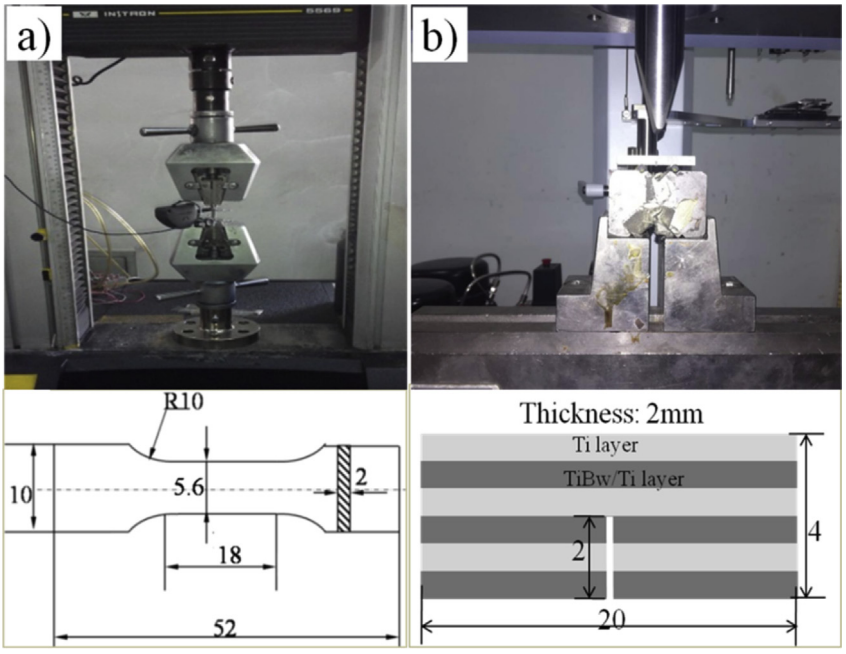

Fig. 2. The testing machines and testing sample dimensions. a) the Instron-5569 tensile testing machine and the general room-temperature tensile sample; b) the Instron-5569 bending testing machine and the general room-temperature three point bending testing sample.

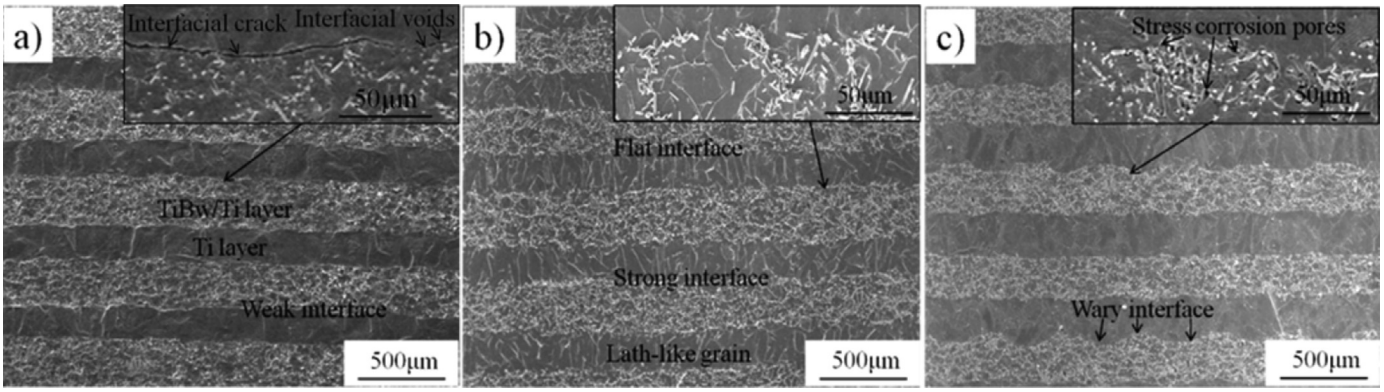

Fig. 3. The microstructures of laminated Ti-(TiBw/Ti) composites fabricated by diffusion welding at different temperatures. a) 1100 °C; b) 1200 °C; c) 1300 °C.

$$\sigma_{TiBw/Ti} = \frac{-E_{Ti}\cdot E_{TiBw/Ti}\left(\alpha_{Ti}-\alpha_{TiB/Ti}\right)\cdot \Delta T}{\left(1-\nu_{TiBw/Ti}\right)E_{Ti}\lambda^{-1}+(1-\nu_{Ti})E_{TiBw/Ti}} \quad (6)$$

where E, ν, α, λ represent Young modulus, Pisson's ratio, thermal expansion coefficient and thickness ratio, respectively. Table 1 lists the physical properties of Ti and TiB phases. Obviously, the residual stresses of two individual layers are gradually increased with increasing fabrication temperature. Moreover, in the TiBw/Ti composite layer, the mismatch between the linear thermal expansion coefficient and elastic modulus in the Ti matrix and TiB whiskers results in the generation of residual stresses in the whiskers and surrounding Ti matrix during cooling after diffusion welding process. There is a residual radial tensile stress and tangential compressive stress surrounding TiB whiskers. The radial matrix stress ($\sigma_{r(Ti)}$) and the tangential matrix stress ($\sigma_{\theta(Ti)} = -\frac{1}{2}\sigma_{r(Ti)}$) is based on the hydrostatic stress ($\sigma_{h(Ti)}$) developed with the whiskers as followed [36]:

Table 1
The physical properties of Ti and TiB [20].

Materials	E (GPa)	α (10^{-6} °C)	ν
Ti	112	9.41	0.3
TiB	427	8.6	0.15

$$\sigma_{r(Ti)} = \sigma_{h(Ti)} = \frac{(\alpha_{Ti}-\alpha_{TiB})\Delta T}{[(1+\nu_{Ti})/2E_{Ti}]+[(1-2\nu_{TiB})/E_{TiB}]} \quad (7)$$

where the subscripts Ti, TiB and TiB/Ti refer to Ti, TiB whisker and TiBw/Ti composite layer, respectively. It is obvious that the residual tensile stresses between Ti matrix and TiB whiskers are gradually increased with increasing fabrication temperature. Therefore, many stress corrosion pores are existed at the interface between Ti matrix and TiB whiskers.

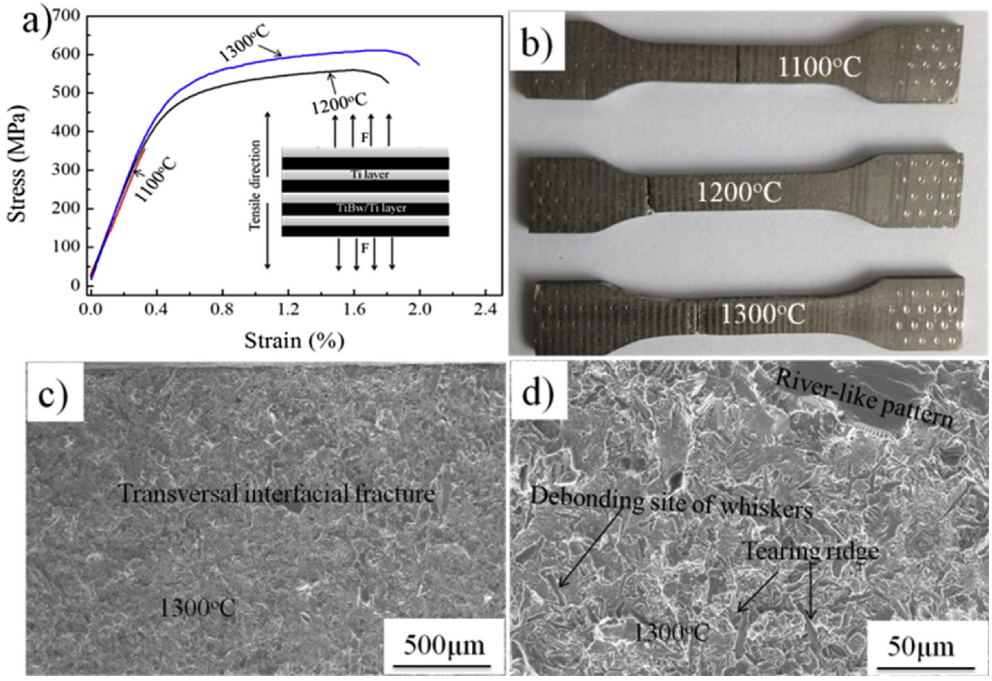

Fig. 4. The transversal tensile stress-strain curves and interfacial fracture morphologies of laminated Ti-(TiBw/Ti) composites. a) transversal tensile stress-strain curves and b) the macroscopic fracture morphology of laminated composites fabricated at different diffusion welding temperatures; transversal interfacial fracture of laminated composites fabricated at 1300 °C c) macroscopic view and d) microscopic view.

The transversal tensile stress-strain curves, fracture morphologies and tensile properties of laminated Ti-(TiBw/Ti) composites are shown in Fig. 4 and Table 2. The laminated composites show gradually increasing transversal tensile strength and tensile ductility with increasing diffusion welding temperatures (Fig. 4a). Fracture zone of three laminated composites are all present in the interface between Ti layer and TiBw/Ti composite layer, and the tensile properties reveal the increasing interfacial bonding strength and interfacial toughness with increasing diffusion welding temperatures. Moreover, the fracture zone of laminated composites fabricated at 1300 °C reveals slight plastic deformation trace as shown in Fig. 4b). Fig. 4c) and d) show the transversal interfacial fracture morphology of laminated composites fabricated at 1300 °C, which reveal that brittle fracture at the interface, intergranular-like fracture accompanied with river-like patterns and tearing ridges initiated by debonded TiB whiskers are shown in Fig. 4c).

The longitudinal tensile stress-strain curves and the tensile properties of laminated Ti-(TiBw/Ti) composites are shown in Fig. 5 and Table 3. The longitudinal tensile properties of laminated composites reveal a complex trend, where the yield strength of the three laminated composites exhibit similar values (552−556 MPa), whereas the ultimate strength and fracture elongation first increase then decrease with increasing diffusion welding temperature. The laminated composites fabricated at 1200 °C exhibit the highest ultimate strength (694 MPa) and fracture elongation (22.7%). Moreover, the laminated composites fabricated at 1100 °C shows a “drop in” phenomenon, which may be attributed to premature interfacial delamination [16], leading to a loss in the load bearing capacity of the individual TiBw/Ti composite layer.

The profile and normal longitudinal fracture characteristics of laminated Ti-(TiBw/Ti) fabricated at different temperatures are shown in Fig. 6. Fig. 6a) shows the macroscopic fracture morphology of laminated composites. Obviously, laminated composites fabricated at 1200 °C obtains the highest fracture

Table 2
The transversal tensile properties and fracture zone of laminated Ti-(TiBw/Ti) fabricated at different temperatures.

Fabrication temperatures (°C)	Tensile strength (MPa)	Tensile elongation (%)	Fracture zone
1100	354 ± 7	–	Interface
1200	559 ± 7	1.8 ± 0.2	Interface
1300	611 ± 8	2.0 ± 0.2	Interface

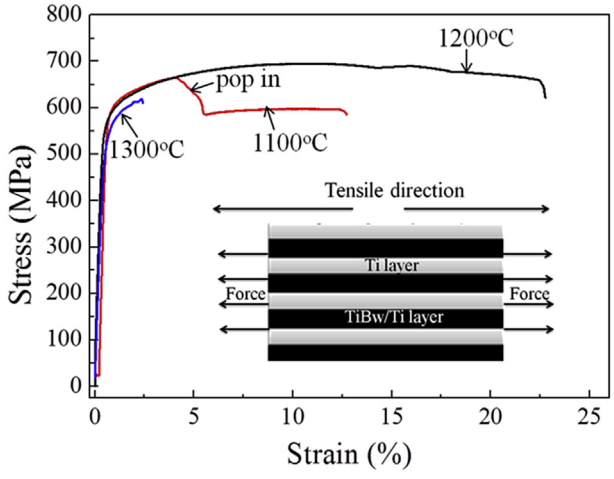

Fig. 5. The longitudinal tensile stress-strain curves of laminated Ti-(TiBw/Ti) composites fabricated at different diffusion welding temperatures.

Table 3
The longitudinal tensile properties of laminated Ti-(TiBw/Ti) fabricated at different temperatures.

Fabrication temperatures (°C)	Yielding strength (MPa)	Tensile strength (MPa)	Tensile elongation (%)
1100	552 ± 3	686 ± 8	12.4 ± 0.2
1200	553 ± 3	694 ± 7	22.7 ± 0.3
1300	556 ± 2	629 ± 8	2.4 ± 0.2

elongation among the three laminated composites. Moreover, the laminated composites fabricated at different temperatures reveal three different fracture characteristics. Fig. 6b) reveals many interfacial delamination cracks due to the low interfacial bonding strength at 1100 °C. There are few micro-cracks in the TiBw/Ti composite layer and many obvious localized shear bands in the Ti layer, which contribute to the fracture ductility. In addition, delamination cracks can induce premature localized necking of the Ti layer as shown in Fig. 6c). Nambu et al. [9,37,38] indicated that interfacial instability occurs before the appearance of diffusion necking emerges and leads to interfacial delamination, which coincides with the critical strain estimated by bifurcation analysis under the plane strain condition. Therefore, occurrence of interfacial delamination leads to non-uniform deformation behavior, such as localized necking, until the sudden rupture of laminated Ti-(TiBw/Ti) composites fabricated at 1100 °C. Fig. 6d) shows that many tunnel cracks and localized shear bands are beneficial for the tensile and bending ductility of the laminated Ti-(TiBw/Ti) composites fabricated at 1200 °C [16]. The main crack reveals that the shear fracture of the Ti layer propagates at nearly 45° along the tensile direction. However, the TiBw/Ti composite layer exhibits tortuous crack propagation path along the network structure of TiB whiskers. The laminated composites do not display interfacial delamination as shown in Fig. 6d) and e), which is attributed to the high interfacial strength (559 MPa) and toughness. Fig. 6f) reveals approximate straight crack propagation paths accompanied with a few micro-cracks, the absence of tunnel and delamination cracks are also observed. Moreover, cleavage fracture is observed in the TiBw/Ti composite layer and lath-like intergranular fracture in the Ti layer as shown in Fig. 6g). These kinds of fracture characteristics are related to the low longitudinal tensile elongation due to the high residual tensile stress.

Fig. 7 shows the fracture schematic diagrams of laminated Ti-TiBw/Ti composites fabricated at 1100 °C, 1200 °C and 1300 °C, respectively. The analysis of delamination crack may be applicable as a criterion given by the following equation [9,37]:

$$K_{interface} \le 0.26 \frac{\pi t_{TiB/Ti} \sigma^2}{2E_{TiB/Ti}} \quad (8)$$

where $E_{TiB/Ti}$ is the Young's modulus of the TiBw/Ti composite layer and $K_{interface}$ is the interfacial toughness. This criterion provides a reasonable means of determining sufficient interfacial toughness to initiate interfacial delamination failure. If the right side of equation (8) is beyond the value of $K_{interface}$ with the increase of longitudinal stress (σ), it can result in delamination fracture. Therefore, the laminated composites fabricated at 1100 °C displays obvious interfacial delamination due to a low interfacial toughness as shown in Fig. 7a). Then the Ti layer and TiBw/Ti composite layer deformed individually with the same tensile strain, tunnel cracks are formed in the TiBw/Ti composite layer, premature localized necking and shear fracture phenomena are presented in the Ti layer, resulting in the serious inhomogeneous plastic deformation behavior and sharp fracture as shown in Fig. 7b).

The schematic diagram of fracture characteristics of laminated

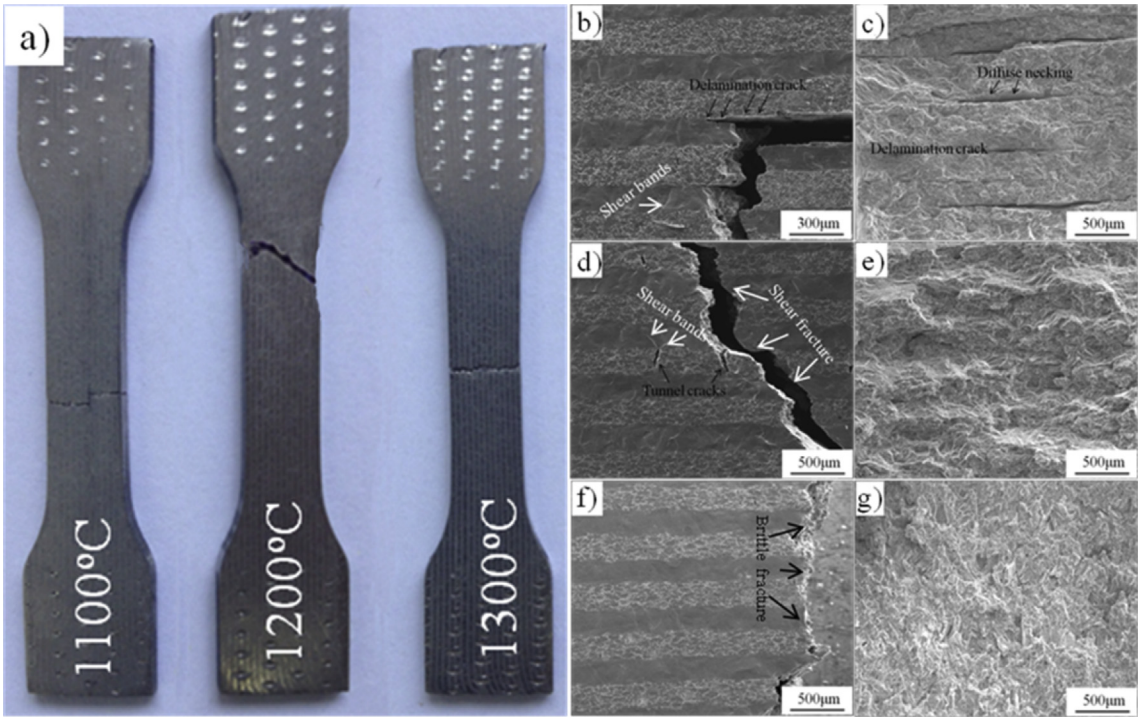

Fig. 6. The fracture characteristics of laminated composites fabricated at different diffusion welding temperatures. a) macroscopic fracture morphology, b), c) 1100 °C; d), e) 1200 °C; f), g) 1300 °C.

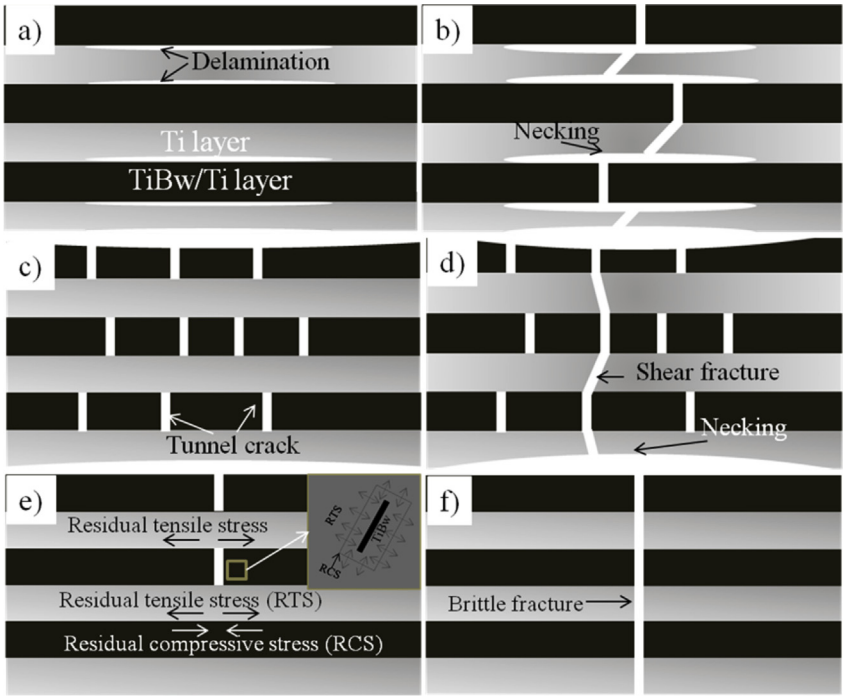

Fig. 7. The schematic diagram of fracture mechanism of laminated Ti-TiBw/Ti composites fabricated at different diffusion welding temperature. a), b) 1100 °C, c), d) 1200 °C, e), f) 1300 °C.

composites fabricated at 1200 °C are shown in Fig. 7c) and d). The high interfacial toughness and interfacial strength are enough to prevent interfacial delamination failure with the increase of longitudinal stress based on equation (8). The localized necking can be effectively delayed by strong interfacial bonding, resulting in the prolong uniform plastic deformation capacity. Herein, many tunnel cracks are formed in the TiBw/Ti composite layer as shown in Fig. 7c). Inoue et al. expressed the following equation for suppressing tunnel crack extension on laminated composites according to the plain strain linear elastic model [37,39]:

$$t_{TiBw/Ti} \leq \frac{4K^2_{IC(TiBw/Ti)}}{\pi\sigma^2} = t_{critical} \quad (9)$$

where $t_{TiB/Ti}$ and $K_{IC(TiB/Ti)}$ are the thickness and fracture toughness of TiBw/Ti composite layer, respectively. $t_{critical}$ is the critical tunnel crack size, and σ is the stress imposed on the TiBw/Ti composite layer. When the thickness of TiBw/Ti composite layer is lower than the critical tunnel crack size, the tunnel crack will be formed and hard to propagate into the Ti layer, which is important in toughening the laminated composites. That is to say, more and more tunnel cracks are present in the TiBw/Ti composite layer with the increase of longitudinal tensile strain. Meanwhile, the Ti layer deformed uniformly with a low stress triaxiality due to slighter localized necking [17]. Finally, one of tunnel cracks propagates into Ti layer until laminated composites can't afford the increasing stress, and the Ti layer reveal obvious shear fracture with about 45° along tensile direction as shown in Fig. 7d).

Residual stress can obviously influent the fracture behavior of laminated composites fabricated at 1300 °C [25]. Residual tensile stress of Ti layer may initiate the fracture characteristics transition from ductile to brittle behavior as shown in Fig. 7e). Moreover, in the TiBw/Ti composite layer, there are super-high residual radial tensile stress presented in the interfaces between Ti matrix and TiB whiskers as shown in the cross picture of Fig. 7e), resulting in premature formation of tunnel cracks. Therefore, the laminated composites fabricated at 1300 °C reveal clear brittle fracture behavior with low fracture strength and elongation as shown in Fig. 7f).

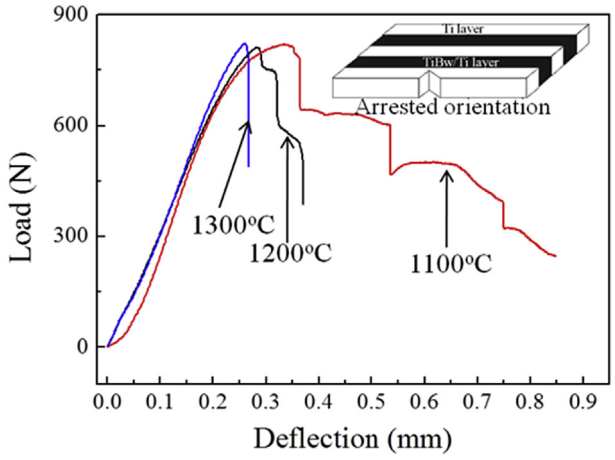

Fig. 8. The bending load-deflection curves of laminated Ti-(TiBw/Ti) composites fabricated at different diffusion welding temperatures.

The bending load-deflection curves of the three laminated Ti-(TiBw/Ti) composites with arrester orientation are shown in Fig. 8. The laminated composites fabricated at 1300 °C only exhibit elastic deformation followed by sudden rupture, revealing the values of maximum load, fracture toughness and fracture work to be 815 N, 10.2 $MPam^{1/2}$ and 27.9 MPam. With the decrease of fabrication welding temperature, the laminated composites reveal obvious "Pop in" fracture behavior and increasing fracture work. The laminated composites fabricated at 1200 °C reveal the values of maximum load, fracture toughness and fracture work to be 811 N, 24.3 $MPam^{1/2}$ and 90.9 MPam, respectively. The laminated composites fabricated at 1100 °C present the highest values of fracture toughness (25.1 $MPam^{1/2}$), fracture work (208.4 MPam) and maximum load (837 N), respectively, which is related to the occurrence of delamination cracks.

Fig. 9 shows the profile bending fracture characteristics of three laminated Ti-(TiBw/Ti) composites fabricated at different diffusion welding temperatures, and the macroscopic fracture morphologies are shown in the cross picture of Fig. 9(a–c). Many interfacial delamination cracks, tunnel cracks and acute localized shear bands are observed in the laminated composites fabricated at 1100 °C as shown in Fig. 9a), which reveal superior fracture toughness and fracture work. Herein, the presence of delamination cracks influences the bending load-displacement relationship, which is according to the Aslan's previous work [40]. However, only few micro-cracks and localized shear bands are present in the laminated composites fabricated at 1200 °C, although the main crack deflects along the interfaces as shown in Fig. 9b). Decreased fracture toughness and fracture work are directly related to the presence of only a straight main crack propagation path, without any other plastic deformation and fracture damage characteristic in the laminated composites fabricated at 1300 °C as shown in Fig. 9c).

Fig. 10 shows an illustration of the fracture process of the laminated Ti-(TiBw/Ti) composites fabricated at 1100 °C with crack arrester orientation. Under the bending condition, the main crack would start advancing along the plane of maximum stress as shown in Fig. 10a). Interfacial delamination occurs ahead of the main crack or when the advancing crack encounters the weak interface between the Ti layer and the Ti-(TiBw/Ti) composite layer as shown in Fig. 10b). The delamination crack makes the main crack difficult to propagate into the next layer, leading to the reduction in the stress

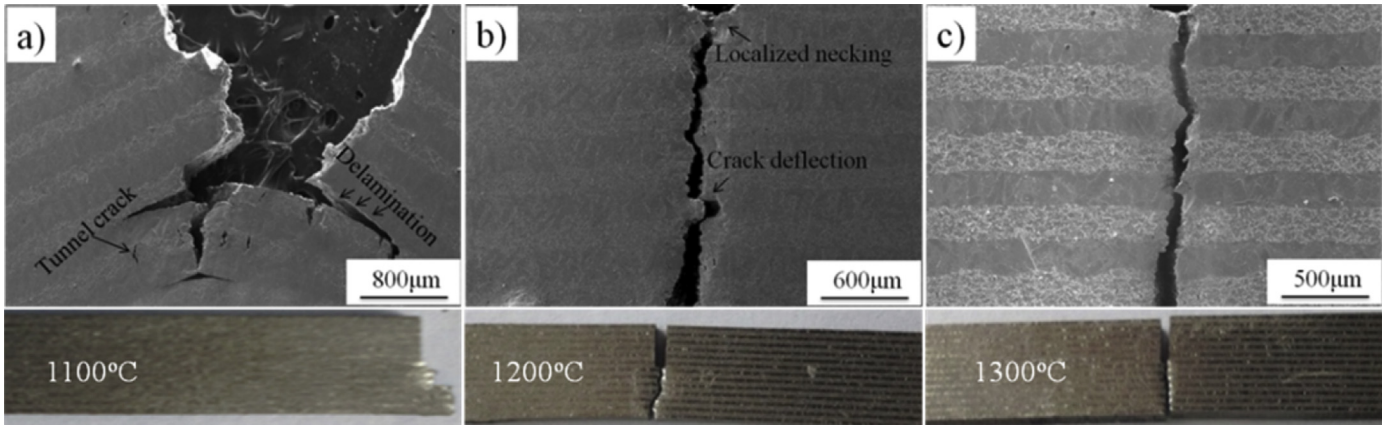

Fig. 9. The profile fracture morphologies of laminated Ti-(TiBw/Ti) composites fabricated at different diffusion welding temperatures with crack arrester orientation. a) 1100 °C; b) 1200 °C; c) 1300 °C.

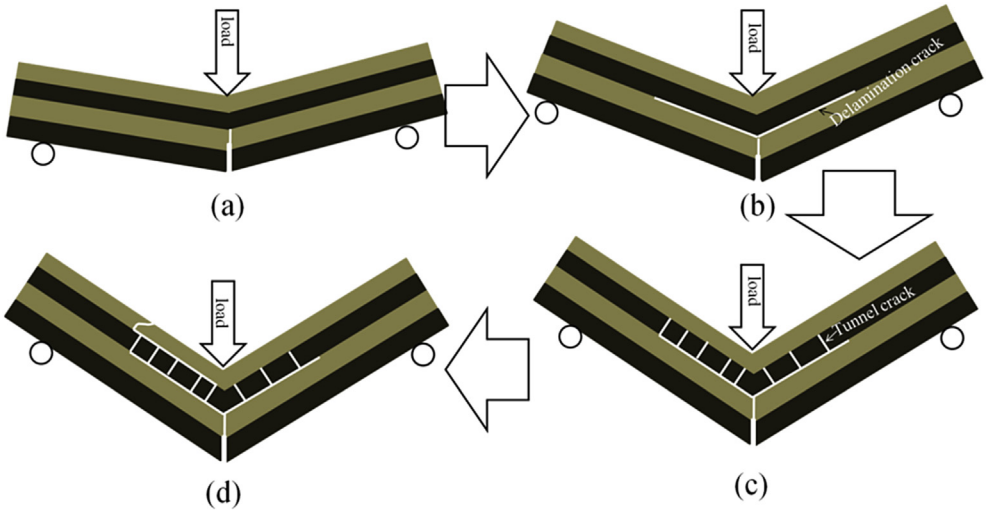

Fig. 10. The illusion graph of bending fracture behavior of laminated Ti-(TiBw/Ti) composites fabricated at 1100 °C. a)-c) fracture process.

intensity of main crack. Thus the main crack replaced by delamination crack moves away from planes of the maximum stress. Then many tunnel cracks are formed in the next TiBw/Ti composite layer, and Ti layer reveals plastic deformation and work hardening behavior as shown in Fig. 10c). According to mechanics of material, the tensile stress is located below the neutral line during the bending process, and the tensile stress in the TiBw/Ti composite layer ($\sigma_{TiBw/Ti}$) can be described by the following equation [41]:

$$\sigma_{TiBw/Ti} = E_{TiBw/Ti} \cdot \varepsilon = E_{TiBw/Ti} \frac{x}{\rho} \tag{10}$$

where x is distance to neutral line and ρ is the radius of curvature, the value of ρ gradually decreases with the increase of displacement, while the value of $\sigma_{TiBw/Ti}$ increases monotonously. Then the tunnel occurs when the value of $\sigma_{TiBw/Ti}$ approaches to the fracture strength of TiBw/Ti composite layer.

More and more tunnel cracks are formed in the following bending deformation process, thus laminated Ti-(TiBw/Ti) composites consume a lot of fracture energy, and then one of tunnel cracks will propagate into the Ti layer due to the increasing stress. Finally, the above steps may be repeatedly carried out until complete failure of the laminated Ti–TiBw/Ti composites. Therefore, the more and longer delamination cracks exist at interfaces, the higher fracture toughness and fracture work are obtained due to presence of more tunnel cracks.

4. Conclusions

(1) Three kinds of laminated Ti-(TiBw/Ti) composites were fabricated at different diffusion welding temperatures of 1100 °C, 1200 °C and 1300 °C. Strong interfacial bonding between layers without pores or voids were obtained at 1200 °C. Many interfacial cracks and interfacial voids were present in the laminated composites fabricated at 1100 °C. However, corrosion pores due to high residual stress are existed in the laminated composites fabricated at 1300 °C;

(2) The interfacial bonding strength and interfacial toughness of the laminated Ti-(TiBw/Ti) composites can be adjusted by controlling the diffusion welding temperature. The transversal tensile strength and tensile elongation gradually increased with increasing diffusion welding temperatures, from 1100 °C to 1300 °C, which is attributed to the gradually increased interfacial bonding;

(3) The laminated Ti-(TiBw/Ti) composites fabricated at 1200 °C exhibited the highest tensile strength and tensile elongation along the longitudinal direction, which is attributed to the strong interfacial bonding. The lowest longitudinal ultimate tensile strength and ductility of the laminated composites fabricated at 1300 °C are attributed to the high residual tensile stress;

(4) The laminated Ti-(TiBw/Ti) composites fabricated at 1100 °C possess the highest fracture toughness and fracture work among the three laminated composites, which is attributed to the delamination cracks and multiple tunnel cracks toughening mechanisms under crack arrester orientation.

Acknowledgements

This work is financially supported by the National Natural Science Foundation of China (NSFC) under Grant Nos. 51601055, 51671068, 51471063 and 51401068, the Hebei Science and Technology program under Grant No. 130000048, the National Natural Science Foundation of Hebei Province under Grant Nos. E201620218 and QN2016029. The Fundamental Research Funds for the Central Universities (Grant No. HIT.BRETIII.201401 and NSRIF. 2014001).

References

[1] Lu WJ, Xiao L, Xu D, Qin JN, Zhang D. Microstructural characterization of Y2O3 in in situ synthesized titanium matrix composites. J Alloys Comp 2007;433:140–6.
[2] Geng L, Ni DR, Zhang J, Zheng ZZ. Hybrid effect of TiBw and TiCp on tensile properties of in situ titanium matrix composites. J Alloys Comp 2008;46:488–92.
[3] Wu H, Jin BC, Geng L, Fan GH, Cui XP, Huang M. Ductile-phase toughening in TiBw/Ti-Ti3Al metallic-intermetallic laminate composites. Metal Mater Trans A 2015;46:3803–7.
[4] Huang LJ, Geng L, Peng HX. In situ (TiBw+TiCp)/Ti6Al4V composites with a network reinforcement distribution. Mat Sci Eng A 2010;527:6723–7.
[5] Fang TH, Li WL, Tao NR, Lu K. Revealing extraordinary intrinsic tensile plasticity in gradient nano-grained copper. Science 2011;331:1587–90.
[6] Wu H, Fan GH, Jin BC, Geng L, Cui XP, Huang M. Fabrication and mechanical properties of TiBw/Ti-Ti(Al) laminated composites. Mater Des 2016;89:697–702.
[7] Liu BX, Huang LJ, Geng L, Kaveendran B, Wang B, Song XQ, et al. Gradient grain distribution and enhanced properties of novel laminated Ti-(TiBw/Ti) composites by reaction hot-pressing. Mater Sci Eng A 2014;595:257–65.
[8] Levi-Sasson A, Meshi I, Mustacchi S, Amarilio I, Benes D, Favorsky V, et al.

Experimental determination of linear an nonlinear mechanical properties of laminated soft composites material system. Compos Part B 2014;57:96–104.
[9] Nambu S, Michiuchi M, Inoue J, Koseki K. Effect of interfacial bonding strength on tensile ductility of multilayered steel composites. Comp Sci Techn 2009;69:1936–41.
[10] Li T, Suo Z. Deformability of thin metal films on elastomer substrates. Int J Solids Struct 2006;43:2351–63.
[11] Zhang XH, Zhou P, Hu H, Han WB. Toughening of laminated ZrB_2-SiC ceramics with residual surface compression. J Eur Ceram Soc 2011;31:2415–23.
[12] Ji G, Ouyang ZY, Li GQ. Effects of bondline thickenss on mode-I nolinear interfacial fracture of laminated composites: an experimental study. Compos Part B 2013;47:1–7.
[13] Zuo KH, Jiang DL, Lin QL. Mechanical properties of Al_2O_3/Ni laminated composites. Mater Lett 2006;60:1265–8.
[14] Cepeda-Jimenez CM, Carreno F, Ruano OA, Sarkeeva AA, Kruglov AA, Lutfullin YR. Influence of interfacial defects on the impact toughness of solid state diffusion bonded Ti-6Al-4V alloy based multilayer composites. Mater Sci Eng A 2013;563:28–35.
[15] Liu BX, Huang LJ, Geng L, Wang B, Cui XP, Liu C, et al. Microstructure and tensile behavior of novel laminated Ti-TiBw/Ti composites by reaction hot pressing. Mater Sci Eng A 2013;583:182–7.
[16] Liu BX, Huang LJ, Geng L, Wang B, Liu C, Zhang WC. Fabrication and superior ductility of laminated Ti-TiBw/Ti composites by diffusion welding. J Alloys Comp 2014;602:187–92.
[17] Liu BX, Huang LJ, Geng L, Wang B, Cui XP. Fracture behaviors and microstructural failure mechanisms of laminated Ti-TiBw/Ti composites. Mater Sci Eng A 2014;611:290–7.
[18] Liu BX, Huang LJ, Wang B, Geng L. Effect of pure Ti thickness on the tensile behavior of laminated Ti-TiBw/Ti composites. Mater Sci Eng A 2014;617:115–20.
[19] Liu BX, Huang LJ, Geng L, Wang B, Cui XP. Effects of reinforcement volume fraction on tensile behaviors of laminated Ti-TiBw/Ti composites. Mater Sci Eng A 2014;610:344–9.
[20] Liu BX, Huang LJ, Geng L. Elastic and plastic behavior of laminated Ti-TiBw/Ti composites. J Wuhan Univ Technol Mater Sci Ed 2015;30:596–600.
[21] Uscinowicz R. Impact of temperature on shear strength of single lap Al-Cu bimetallic joint. Compos Part B 2013;44:344–56.
[22] Uscinowicz R. Experimental identification of yield surface of Al-Cu bimetallic sheet. Compos Part B 2013;55:96–108.
[23] Liu BX, Huang LJ, Rong XD, Geng L, Yin FX. Bending behaviors and fracture characteristics of laminated ductile-tough composites under different modes. Compos Sci Technol 2016;126:94–105.
[24] Atrian A, Fereshteh-Saniee F. Deep drawing process of steel/brass laminated sheets. Compos Part B 2013;47:75–81.
[25] Akpinar S. The strength of the adhesively bonded step-lap joints for different step numbers. Compos Part B 2014;67:170–8.
[26] Sheng LY, Yang F, Xi TF, Lai C, Ye HQ. Influence of heat treatment on interface of Cu/Al bimetal composite fabricated by cold rolling. Compos Part B 2011;42:1468–73.
[27] Zuo KH, Jiang DL, Lin QL, Zeng YP. Improving the mechanical properties of Al_2O_3/Ni laminated composites by adding Ni particles in Al_2O_3 layers. Mater Sci Eng A 2007;443:296–300.
[28] Song JJ, Zhang YS, Fang Y, Fan HZ, Hu LT, Qu JM. Influence of structural parameters and transition interface on the fracture properties of Al_2O_3/Mo laminated composites. J Eur Soc 2015;35:1581–91.
[29] Huang LJ, Geng L, Xu HY, Peng HX. In situ TiC particles reinforced Ti6Al4V matrix composite with a network reinforcement architecture. Mater Sci Eng A 2011;528:2859–62.
[30] Steif PS. Interfacial instabilities in an unbonded layered solid. Int J Solids Struct 1990;26:915–25.
[31] Hutchinson JW. Necking modes in multilayers and their influence on tearing toughness. Math Mech Solids 2014;19:39–55.
[32] Bigoni D, Needleman A. Effect of interfacial compliance on bifurcation of a layer bonded to a substrate. Int J Solids Struct 1997;34:4305–26.
[33] Yu HL, Tieu AK, Lu C, Liu X, Godbole A, Li HJ, et al. A deformation mechanism of hard metal surrounded by soft metal during roll forming. Sci Rep 2014;4:5017.
[34] Eizadiou M, Talachi AK, Manesh HD, Shahabi HS, Janghorban K. Investigation of structure and mechanical properties of multi-layered Al/Cu composite produced by accumulative roll bonding (ARB) process. Compos Sci Technol 2008;68:203–2009.
[35] Zhang XH, Zhou P, Hu P, Han WB. Toughening of laminated ZrB2-SiC ceramics with residual surface compression. J Eur Ceram Soc 2011;31:2415–23.
[36] Wei GC, Becher PF. Improvements in mechanical properties in SiC by the addition of TiC particles. J Am Ceram Soc 1984;67:571–4.
[37] Koseki T, Inoue J, Nambu S. Development of multilayer steels for improved combinations of high strength and high ductility. Mater Trans 2014;55:227–37.
[38] Steif PS. Bimaterial interface instabilities in plastic solids. Int J Solids Struct 1986;22:195–207.
[39] Inoue J, Nambu S, Ishimoto Y, Koseki T. Fracture elongation of brittle/ductile multilayered steel composites with a strong interface. Scripta Materialia 2008;59(10):1055–8.
[40] Aslan Z, Daricik F. Effect of multiple delaminations on the compressive, tensile, flexural, and buckling behavior of E-glass/epoxy composites. Compos Part B 2016;100:186–96.
[41] Sun YB, Chen J, Ma FM, Ameyama K, Xiao WL, Ma CL. Tensile and flexural properties of multilayered metal/intermetallics composites. Mater. Charac 2015;102:165–72.